

- 171 (1973); W. J. Greeney, D. A. Bella, H. Curl, *ibid.*, p. 405.
7. R. Petersen, *ibid.* 109, 35 (1975).
  8. R. W. Eppley and W. H. Thomas, *J. Phycol.* 5, 375 (1969); R. R. L. Guillard, P. Kilham, T. A. Jackson, *ibid.* 9, 233 (1973).
  9. *Asterionella formosa*, S. S. Kilham's clone Frains AF, was isolated from Frains Lake, Mich.; *C. meneghiniana*, clone CyOHF2, was isolated from Lake Ohrid, Yugoslavia, by S. S. Kilham and obtained in axenic condition by V. McAlister.
  10. Light-dark cycle of 12 : 12, light from fluorescent bulbs at about  $100 \mu\text{ein m}^{-2} \text{sec}^{-1}$ ;  $20^\circ \pm 0.5^\circ\text{C}$ ; algal medium WC, described by R. R. L. Guillard and C. J. Lorenzen [*J. Phycol.* 8, 10 (1972)].
  11. J. W. G. Lund, F. J. H. Mackereth, C. H. Mortimer, *Philos. Trans. R. Soc. London Ser. B* 246, 255 (1963); C. F. Powers, D. W. Schults, K. W. Malueg, R. M. Brice, M. D. Schuldt, in *Nutrients and Eutrophication*, G. E. Likens, Ed. (American Society of Limnology and Oceanography, Lawrence, Kan., 1971), pp. 141-156; C. L. Schleske and E. F. Stoermer, *Science* 173, 423 (1971).
  12. P. Kilham, *Limnol. Oceanogr.* 16, 10 (1971).
  13. R. C. Dugdale, *ibid.* 12, 605 (1967).
  14. Unpublished results obtained with S. S. Kilham. Culture flasks of WC medium (10) were inoculated with nutrient-starved cells at a density of about 500 cells per milliliter, and allowed to grow for 4 days, with cell counts made daily. Initial nutrient concentrations did not decrease more than 25 percent by day 4 because of the low cell density at the start of the experiments. Growth rate at each initial concentration was estimated by a least-squares linear regression of logarithm to base 2 of cell counts versus day. These data were fitted to the Michaelis-Menten equation by a nonlinear regression [by the method of C. I. Bliss and A. T. James, *Biometrics* 22, 573 (1966)] which provides confidence limits about the mean.
  15. A *t*-statistic was used to test significant differences of all means with significance stated.
  16. Both  $\text{PO}_4$  uptake and  $\text{PO}_4$ -limited growth rates at various concentrations of  $\text{PO}_4$  are needed to make this conclusion. Short-term (batch)  $\text{PO}_4$  uptake experiments with both species, cultured singly, revealed no significant differences ( $P > .95$ ) in *K* or in the maximal rate of  $\text{PO}_4$  uptake between the two species. Because uptake abilities are not significantly different, the species best able to convert low  $\text{PO}_4$  levels into growth should be the superior competitor.
  17. The  $\text{SiO}_2$  uptake experiments revealed no significant differences in *K* or in the maximal rate of  $\text{SiO}_2$  uptake between the two species. Thus, *C. meneghiniana* should be the competitive dominant when both species are limited by  $\text{SiO}_2$ .
  18. M. R. Droop, *J. Mar. Biol. Assoc. U.K.* 54, 825 (1974); G.-Y. Rhee, *J. Phycol.* 10, 470 (1974).
  19. Nutrient ratios are employed here for ease of presentation of experimental results. Under controlled culture conditions in which only specific nutrients may be limiting growth rate, use of ratios should be valid. For natural situations, absolute concentrations and supply (turnover) rates of all relevant nutrients should be used.
  20. I present this simple model of steady-state competition to illustrate the potential power of resource utilization theory. Numerous other interpretations, based on more physiologically realistic models, are possible and are in preparation. This model illustrates what may be an essential aspect of any resource-based model: stable, steady-state coexistence occurs only when the growth rate of each species is limited by a different resource.
  21. The ratio of  $\text{SiO}_2$  to  $\text{PO}_4$  in the influent medium was adjusted as shown (Fig. 2). This approximates steady-state concentration ratios for which the simple mathematical analysis presented is valid. In all cases, the absolute concentrations of  $\text{PO}_4$  and  $\text{SiO}_2$  were low enough that only  $\text{SiO}_2$  or  $\text{PO}_4$  should be limiting growth rate. Cultures were diluted manually daily by removing a portion and replacing it with medium. Flow rates are expressed as the ratio of the volume removed per day to the total culture volume.
  22. A species was considered competitively displaced when it comprised less than 5 percent (by number of cells) in a mixed species culture. Mixed cultures were started with each species in equal abundance.
  23. These cultures showed no shift in the proportions of each species between about day 20 and day 42, when experiments were generally terminated.
  24. R. Levins, *Evolution in Changing Environments* (Princeton Univ. Press, Princeton, N.J., 1968).
  25. To directly apply this work to a lake, it is necessary to know that ambient concentrations

are at steady state and to experimentally demonstrate that  $\text{SiO}_2$  and  $\text{PO}_4$  are limiting growth rate. If these conditions hold, *C. meneghiniana*, for instance, should be increasingly dominant (relative to *A. formosa*) as  $[\text{SiO}_2]/[\text{PO}_4]$  decreases below 5.6, given sufficient time for steady-state conditions to prevail.

26. J. T. Lehman, D. B. Botkin, G. E. Likens, *Limnol. Oceanogr.* 20, 343 (1975).
27. Supported by a University of Michigan Rack-

ham predoctoral fellowship to D.T. and by NSF grant GB-41315 to P. Kilham, I thank P. Kilham, S. S. Kilham, J. Adams, J. Porter, D. Wethey, B. Hazlett, J. Vandermeyer, and a reviewer for comments and C. Kott for assistance with experiments. This work is part of a dissertation submitted in partial fulfillment of the Ph.D. degree at the University of Michigan.

24 September 1975; revised 19 December 1975

## Potassium-Argon Ages from the Galápagos Islands

**Abstract.** Potassium-argon ages of eight volcanic rocks from some of the geologically oldest flows exposed in the Galápagos Archipelago indicate that the Galápagos Islands have a probable maximum age of 3 million years. Rocks from six islands were dated; the oldest are from Española ( $3.2 \pm 0.2$ ), Santa Fe ( $2.7 \pm 0.1$ ), and Plazas ( $4.2 \pm 1.8$  million years). The new data suggest that the Galápagos Islands are younger than previously supposed on the basis of marine magnetic anomaly dating, but they are older than most previously dated rocks from the Galápagos.

The Galápagos Islands have been of interest to biologists since 1835, when Darwin (1) noted their relative isolation from any major land mass, their geologic youthfulness, and the differentiation of species on and within the island archipelago. The age of the islands is important to any biological, evolutionary, geo-

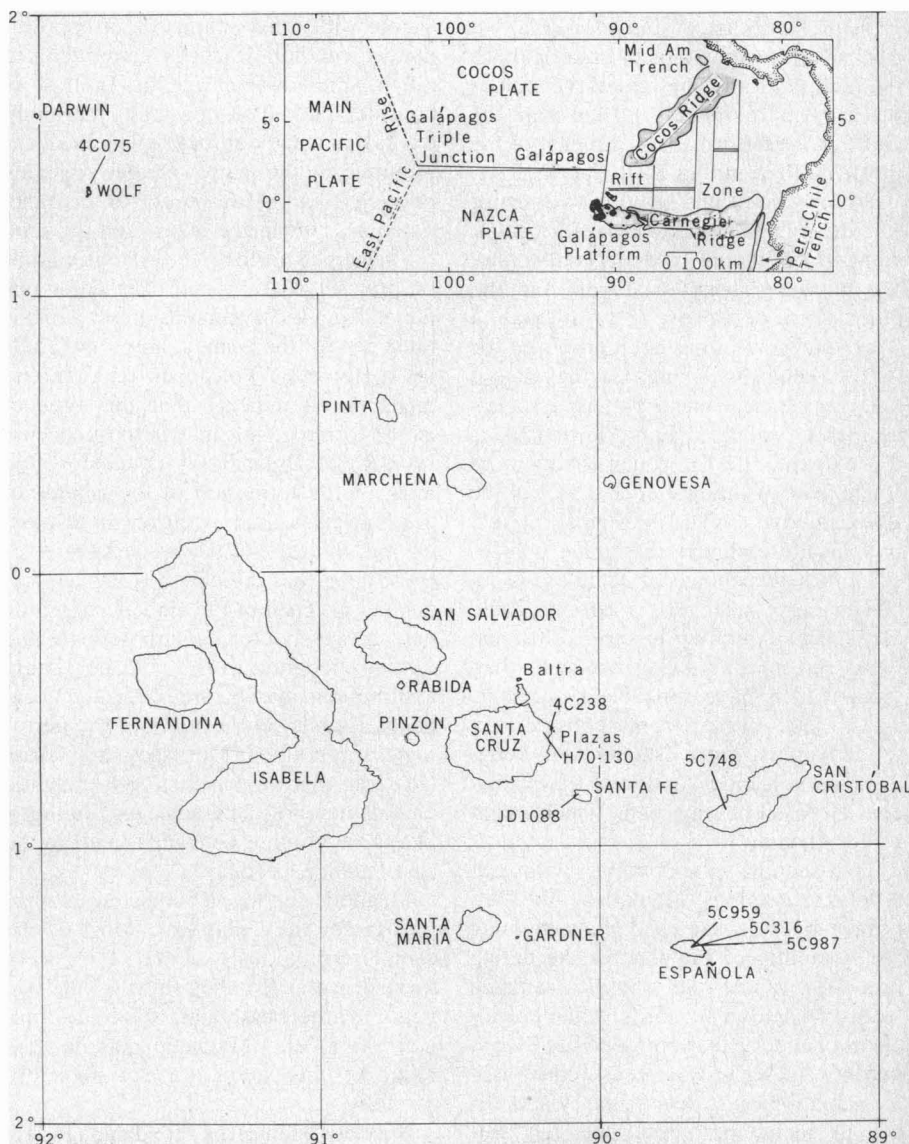


Fig. 1. Galápagos Islands. Sample sites are indicated by numbers (see Table 1). The inset shows schematically the major tectonic features that surround the Galápagos Islands (15).

Table 1. Potassium-argon ages of volcanic rocks from the Galápagos Islands. Methods used to determine  $K_2O$  were isotope dilution (ID) and flame photometry (F). Calculations were based on decay constants  $\lambda_e = 0.585 \times 10^{-10} \text{ year}^{-1}$  and  $\lambda_\beta = 4.72 \times 10^{-10} \text{ year}^{-1}$  and on  $^{40}K/K_{\text{total}} = 1.19 \times 10^{-4}$ .

| Sample  | Island        | Material    | Weight (g) | $K_2O$ (weight percent) | Argon-40 |                                 | Age (million years) |
|---------|---------------|-------------|------------|-------------------------|----------|---------------------------------|---------------------|
|         |               |             |            |                         | Percent  | Total ( $\times 10^{-11}$ mole) |                     |
| 4C075   | Wolf          | Basalt      | 6.7192     | 0.3717 (ID)             | 0.7      | 0.2666                          | $0.72 \pm 1.1$      |
| H70-130 | Santa Cruz    | Plagioclase | 10.8040    | 0.0596 (ID)             | 1.6      | 0.0987                          | $1.03 \pm 0.78$     |
|         |               |             | 11.4620    | 0.0600 (ID)             | 2.3      | 0.0992                          | $0.98 \pm 0.43$     |
| 4C238   | Plazas        | Plagioclase | 8.4949     | 0.0412 (F)              | 6.7      | 0.2180                          | $4.2 \pm 1.8$       |
| JD1088  | Santa Fe      | Basalt      | 21.5895    | 0.645 (F)               | 33.0     | 5.790                           | $2.85 \pm 0.06$     |
|         |               |             | 24.0029    | 0.653 (F)               | 25.7     | 5.785                           | $2.56 \pm 0.08$     |
|         |               |             |            | 0.623 (F)               |          |                                 |                     |
|         |               |             |            | 0.623 (F)               |          |                                 |                     |
| 5C748   | San Cristóbal | Basalt      | 8.0272     | 0.6072 (ID)             | 8.1      | 0.42725                         | $0.66 \pm 0.08$     |
| 5C959   | Española      | Basalt      | 6.3055     | 0.986 (ID)              | 22.2     | 2.791                           | $3.04 \pm 0.11$     |
| 5C316   | Española      | Basalt      | 7.1784     | 0.373 (ID)              | 6.2      | 0.8410                          | $2.12 \pm 0.38$     |
| 5C987   | Española      | Basalt      | 5.5238     | 0.377 (ID)              | 8.6      | 1.019                           | $3.31 \pm 0.36$     |

logical, or geophysical study of the Pacific Ocean basin. Potassium-argon dating of rocks from several of the islands was therefore done.

The Galápagos island group lies near the equator, approximately 1000 km west of the coast of Ecuador (Fig. 1). The islands are the tops of basaltic (both tholeiitic and alkaline) shield volcanoes that rise approximately 1.5 km from the Galápagos platform, 1200 km east of the north-south trending East Pacific Rise.

Within the island group two major fracture systems characterize the alignment of individual calderas and faults; one of these strikes east-west and the other north-northwest (2). Although a "hot spot" origin has been proposed for the Galápagos Islands (3), they do not fall into the clear linear pattern associated with some other Pacific Ocean islands (for example, the Hawaiian chain).

The date of the first appearance of the islands above the sea is of most interest biologically and was the prime consideration in the choice of samples. Eight basalts were selected for dating (Table 1). Islands exhibiting historic volcanism were rejected as being younger than those which have long been dormant. The rocks were from considerably eroded areas, from islands with long-dormant volcanoes, and from flows adjacent to fossil-bearing beds which might be correlated (4).

Thin-section examination, with criteria discussed by Mankinen and Dalrymple (5), was also used in determining the suitability of samples for the dating process. Whole-rock basalt samples were analyzed in six cases, while plagioclase phenocrysts were separated from two flows. Argon was measured by isotope dilution mass spectrometry according to techniques described by Dalrymple and Lanphere (6). Potassium measurements were done by flame photom-

etry with lithium metaborate fusion (7) and by isotope dilution with a  $^{40}K$ - $^{41}K$  tracer.

The dates obtained are presented in Table 1 and the location of each sample is shown in Fig. 1. All the data are consistent with a maximum age of approximately 3 million years (the error factor in the 4.2-million-year age in Table 1 is considerable). The possibility certainly exists that still older rocks might be deeply buried by the many volcanic episodes on each island. Also, several of the rocks dated are submarine lavas, and the time of their uplift to form the islands cannot be precisely determined. The dates obtained from these samples do set a maximum age for the islands, however. Studies of tholeiitic volcanism on other islands (8, 9) indicate that this type of island-forming volcanic activity occurs rapidly. McDougall (9) concludes that most of the formation of the islands in the Hawaiian chain occurred in at most 0.5 million years. Similarly, Jackson *et al.* (8) assume that the oldest K-Ar age calculated for each of the Hawaiian Islands may be considered to approximate the date of inception of the volcano. These assumptions may be applied to the Galápagos Islands on the basis of the petrologic similarities; McBirney and Aoki (10) note that the basalts (both tholeiitic and alkaline) of the Galápagos are much like those of other volcanic islands in the east Pacific Ocean.

Magnetic studies also indicate a youthful age for the Galápagos. Most of the samples previously dated (11) were formed in the Brunhes (0 to 0.7 million years) or the Matuyama (0.7 to 2.4 million years) era. Magnetic data for the rocks of this study are not presently available.

Previous studies of the Galápagos region are consistent with the K-Ar ages presented here. Anderson *et al.* (12) find,

near the Cocos Ridge, magnetic anomalies which may have formed at the western part of the Galápagos Rift Zone 4 to 9 million years ago. They also identify 10-million-year-old magnetic anomalies from the eastern portion of the Galápagos Rift Zone. However, they hypothesize that an area of crustal melting, which originated 3 to 4 million years ago, was responsible for the creation of the Galápagos Islands and part of the Carnegie Ridge. Herron (13) presents marine magnetic evidence that the East Pacific Rise shifted 800 km westward 9 million years ago to its present site. She feels that this shift initiated processes which resulted in the creation of the Galápagos Islands and the sea floor in that area, and that the Cocos and Nazca plates were created at approximately the same time from the Farallon Plate and then began their present relative motion. Magnetic and K-Ar studies of three of the more central islands (14) (San Salvador, Rabida, and Pinzon) indicate no evidence for ages greater than approximately 1 million years.

There is no clear trend of the K-Ar ages of this study comparable to that observed for the Hawaiian Island chain (8). However, the Galápagos Islands are small compared to Hawaii, and available dates are sparse, making identification of any trends most difficult.

KIMBERLY BAILEY

U.S. Geological Survey,  
Pacific-Arctic Branch of  
Marine Geology,  
345 Middlefield Road,  
Menlo Park, California 94025

#### References and Notes

1. C. Darwin, *The Voyage of the Beagle* (Doubleday, New York, 1962), pp. 373-401.
2. A. R. McBirney and H. Williams, *Geol. Soc. Am. Mem.* 118 (1969).
3. W. J. Morgan, *Am. Assoc. Pet. Geol. Bull.* 56, 203 (1972).
4. A. Cox, H. Williams, K. Howard, G. B. Dalrymple, personal communications.

5. E. Mankinen and G. B. Dalrymple, *Earth Planet. Sci. Lett.* **17**, 89 (1972).
6. G. B. Dalrymple and M. A. Lanphere, *Potassium-Argon Dating: Principles, Techniques and Applications to Geochronology* (Freeman, San Francisco, 1969).
7. C. O. Ingamells, *Anal. Chim. Acta* **52**, 323 (1970).
8. E. O. Jackson, E. A. Silver, G. B. Dalrymple, *Geol. Soc. Am. Bull.* **83**, 601 (1972).
9. I. McDougall, *ibid.* **75**, 107 (1964).
10. A. R. McBirney and K. Aoki, in *The Galápagos*, R. I. Bowman, Ed. (Univ. of California Press, Berkeley, 1966).
11. A. V. Cox and G. B. Dalrymple, *Nature (London)* **209**, 776 (1966).
12. R. N. Anderson, D. A. Clague, K. D. Klitgord, M. Marshall, R. K. Nishimori, *Geol. Soc. Am. Bull.* **86**, 683 (1975).
13. E. M. Herron, *Geol. Soc. Am. Bull.* **83**, 1671 (1972).
14. F. J. Swanson, H. W. Baitis, J. Lexa, J. Dymond, *ibid.* **85**, 1803 (1974).
15. T. H. Van Andel, G. R. Heath, B. T. Malfait, D. F. Heinrichs, J. I. Ewing, *ibid.* **82**, 1489 (1971).
16. Potassium-argon dating was done at the U.S. Geological Survey, Menlo Park, under the direction of G. B. Dalrymple, who also reviewed the manuscript. A. L. Berry and S. J. Kover assisted with the argon and potassium measurements. J. R. Sulat provided computer programming. A. V. Cox collected most of the samples; his comments and field notes were helpful. Further samples and pertinent information came from G. B. Dalrymple, H. Williams, J. W. Durham, and K. A. Howard.

17 November 1975; revised 29 January 1976

## Differing Attenuation Coefficients of Normal and Infarcted Myocardium

**Abstract.** *There are significant differences in attenuation coefficients between normal and infarcted myocardium measurable with a computerized transaxial tomographic scanner. Additionally, iodinated contrast material administered prior to killing the test animals resulted in excellent visualization of the blood-myocardial interface at a time when standard radiographs detected no differences between the ventricular cavity and the myocardial wall. These natural and induced changes in attenuation coefficients offer a new approach to evaluating and understanding the processes of tissue injury and death. Their clinical relevance lies in application to the twin problems of myocardial infarction and the structure and function of the cardiac wall.*

The accurate detection and sizing of infarcted myocardium is of major experimental and clinical importance. It represents an essential step in developing an in vivo approach to the study of tissue infarction and necrosis. In the clinical setting, it not only permits the diagnosis of acute infarction but also is vital in evaluating interventions designed to limit the degree to which ischemic heart muscle goes on to cellular death (1).

At present, the most useful approach to visualizing the volume of infarcted tissue employs radionuclides (2, 3). This method is limited by both image resolution and heterogeneous tissue uptake of the isotope. Current methods of delineating the cardiac chambers generally employ invasive intracardiac catheterization and the rapid delivery of an iodinated contrast agent, recorded serially on cine or large film. Noninvasive methods, such as radionuclide imaging and echocardiography, have significant limitations of resolution and extent of visualization.

The delineation of normal and abnormal myocardium and visualization of the cardiac chambers could be readily accomplished by noninvasive means if there were detectable differences in x-ray absorption by normal myocardium, ischemic or dead myocardium, and the intracavitary blood pool. In this study we evaluated whether the differing tissue compositions were adequate to register altered images on computerized trans-

axial tomograms (CTT) and the degree to which physiologic doses of contrast agent might enhance visualization of the myocardial wall.

Five normal mongrel dogs weighing 14 to 20 kg were killed immediately after receiving, intravenously, 5000 units of aqueous heparin. In addition, one of these animals had received 1.0 ml/kg of a mixture of meglumine and sodium diatrizoate (37 percent iodine) (Renografin-76, E. R. Squibb & Sons, Princeton, N.J.) 5 minutes prior to death. Acute myocardial infarctions were created in four similar dogs by embolization of a radiopaque polyethylene plug into the left anterior descending coronary artery under fluo-

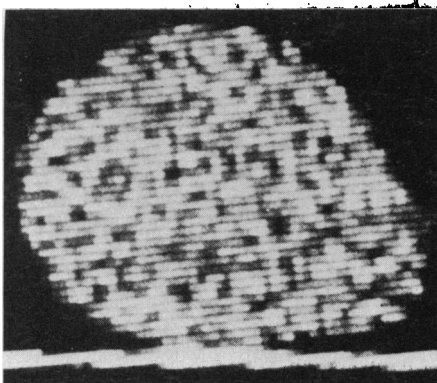


Fig. 1. Normal heart with no contrast agent given. Section at ventricular level showing uniform absorption with a value for myocardium of  $26.0 \pm 0.6$  EMI units and for blood of  $26.2 \pm 1.0$  EMI units.

roscopic control (2). Two days later, 5000 units of aqueous heparin were administered intravenously and the animals were killed immediately. The hearts of all nine dogs were excised after ligation of the venae cavae, the hilar pulmonary arteries and veins, and the aorta. The excised hearts were shaken and placed in a divided plastic container (Tupperware Corp., Orlando, Fla.) which was filled with 0.9 percent sodium chloride and fitted snugly into the head cap of the EMI (EMI Medical Inc., Northbrook, Ill.) CTT scanner. The specimens were scanned at 120 or 140 kv; the scan thickness was either 8 or 13 mm. Attenuation coefficients were measured with the EMI scanner, which has a 160 by 160 matrix and has previously been described in detail (4-7).

Scans of representative areas of myocardial wall in normal hearts had uniform EMI values of  $26.0 \pm 0.6$  EMI units (mean  $\pm$  standard error of the mean). In these animals the intracavitary blood values were  $26.2 \pm 1.0$  EMI units. [One EMI unit corresponds to approximately a 0.2 percent difference in x-ray attenuation coefficient compared to water (7)]. There was no consistent visualization of the myocardial-blood interface (Fig. 1). When the hearts were allowed to stand for a protracted interval, the red blood cells settled to the lower portion of the ventricular cavity, which became denser than the myocardial wall, while the plasma in the upper portion of the cavity was less dense.

The administration of contrast agent to the animals before they were killed resulted in a cavitory (blood pool) attenuation coefficient of  $43 \pm 1$  EMI units, compared to a myocardial attenuation coefficient of  $33 \pm 1$  EMI units, with consequent clear visualization of the blood-myocardial wall interface (Fig. 2). This difference of 10 EMI units corresponds to about 2 percent difference in the attenuation coefficients of intracavitary blood and myocardial wall. Despite the measurable difference in attenuation coefficient, high-quality, low-kilovoltage standard radiographs taken immediately after scanning failed to demonstrate any detectable difference in radiographic density between the myocardial wall and intracavitary blood.

The animals with myocardial infarctions showed three different scan patterns. In two animals the site of histologically confirmed infarction displayed attenuation coefficients 1 percent lower than in the surrounding normal myocardium (for example, infarct,  $21.7 \pm 1.2$  EMI units compared to normal myocardium,  $26.8 \pm 1.0$  EMI units) (Fig. 3a). In a third animal the attenuation coefficient



## Potassium-Argon Ages from the Galápagos Islands

Kimberly Bailey

*Science* **192** (4238), . DOI: 10.1126/science.192.4238.465

### View the article online

<https://www.science.org/doi/10.1126/science.192.4238.465>

### Permissions

<https://www.science.org/help/reprints-and-permissions>